



Crystal structure of a protein–aromatic foldamer composite: macromolecular chiral resolution†

 Cite this: *Chem. Commun.*, 2019, 55, 11087

 Received 11th July 2019,
 Accepted 21st August 2019

DOI: 10.1039/c9cc05330a

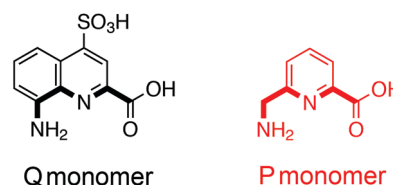
rsc.li/chemcomm

 Jimi M. Alex,^{id}^a Valentina Corvaglia,^{id}^{bc} Xiaobo Hu,^b Sylvain Engilberge,^{id}^a
 Ivan Huc^{id}^{*bc} and Peter B. Crowley^{id}^{*a}

Co-crystallization of a 2 kDa tether-free sulfonated foldamer and the 13 kDa lysine-rich cytochrome c yielded a remarkable biohybrid assembly with chiral resolution of the foldamer helix handedness. In the crystal a ~5 nm foldamer stack was surrounded by eight molecules of protein. NMR and CD experiments suggest interesting differences in the solution state recognition processes.

Supramolecular chemistry provides a repertoire of abiotic synthetic receptors and ligands for protein recognition and assembly.¹ These properties have been illustrated for calixarenes,² cucurbiturils,³ aromatic foldamers,⁴ suramin⁵ and tweezers,⁶ all of which complement medchem products and peptidomimetics. Among the supramolecular components, foldamers are unique in that they form stably-folded architectures in solution.⁷ This feature, arising from their resemblance to biopolymers, makes them attractive candidates for protein recognition.⁸ Currently, there is growing interest in helical aromatic oligoamides.⁹ The stability, fold predictability and ease of synthesis/functionalization of these foldamers have led to a wide range of applications.^{9b,10}

Aromatic foldamers can be customized to enhance biocompatibility. For example, oligoamides of 8-amino-2-quinoline carboxylic acid (Q, Scheme 1) were decorated with proteinogenic side chains.^{4b} Additionally, they can be endowed with a tether functionality that confines the foldamer to a specific region of a protein surface, enabling identification of weak interactions.^{4b,d,11} Thus, foldamers with a benzenesulfonamide were anchored to the active site of human carbonic anhydrase II (HCA), to facilitate



Scheme 1 General structures of amino acid quinoline (Q) and pyridine (P) monomers, and sequences of helical oligoamide foldamers **1** and **2**. The inner rim of the helix is marked in bold.

recognition and assembly,^{4b,d,g} while others were linked to cyclophilin A or interleukin 4.¹¹ The *ab initio* design of foldamers (without a tether) that can bind proteins is a challenging task owing to the dearth of molecular recognition information. Taking inspiration from the charge–charge multivalent complexation between a cationic quinoline oligoamide and a DNA G-quadruplex,¹² the present work was carried out with the objective to demonstrate tether-free foldamer binding to a protein.

We explored the recognition properties of an anionic helical quinoline oligoamide with a lysine-rich protein. The foldamer was a ~2 kDa octamer spanning three helix turns and functionalized with sulfonate groups (**1**, Scheme 1). **1** could be synthesized readily on solid phase using previously reported procedures.¹³ The choice of sulfonic acid was motivated by its suitability to interact with cationic residues.^{2b–d,5,14} Cytochrome *c* (cyt *c*, ~13 kDa, pI ~9) was selected as its interactions with anionic receptors such as sulfonato-, phosphonomethyl- and phosphonato-calix[*n*]arenes are well-established.^{2,14,15}

A 2.1 Å resolution crystal structure provided a detailed view of the protein–foldamer composite.¹⁶ Remarkably, the co-crystal resulted in the chiral resolution of the *P* and *M* helices of **1**, the interconversion of which is kinetically hampered. NMR studies were performed to characterize complexation in solution. Circular dichroism (CD) experiments with **2**, an analogue of **1** containing

^a School of Chemistry, National University of Ireland, University Road, Galway, H91 TK33, Ireland

^b Université de Bordeaux, CNRS, Bordeaux Institut National Polytechnique, CBMN (UMR 5248), Institut Européen de Chimie et Biologie, 2 Rue Escarpit, Pessac 33600, France

^c Department of Pharmacy and Center for Integrated Protein Science, Ludwig-Maximilians-Universität, Butenandtstraße 5-13, München 81377, Germany.
 E-mail: ivan.huc@cup.lmu.de, peter.crowley@nuigalway.ie;
 Tel: +49 89 218 077 804, +353 91 49 24 80

† Electronic supplementary information (ESI) available: Methods, characterisation of new compounds and X-ray statistics table. See DOI: 10.1039/c9cc05330a

flexible aminomethyl-pyridine units (P, Scheme 1), provided insight into helix handedness induction by the protein.¹⁷

Crystallization trials were performed with the Jena Bioscience JCSG++ screen and an Oryx 8 robot. Crystals of *cyt c* - **1** grew only in condition C7, containing 10% PEG 3000, 0.1 M sodium acetate pH 4.5 and 0.2 M zinc acetate. Similar conditions B7 and D4, lacking zinc, did not yield crystals. Rod-like crystals (Fig. 1) were reproducible with 5–25% PEG 3350 and 4 eq. of **1** prepared in 1 M sodium acetate. Thin plate co-crystals were obtained with **1** or **2**, prepared in pure water, but they diffracted poorly to > 4 Å resolution. Data extending to 2.1 Å resolution was collected (SOLEIL synchrotron) from the rod-like *cyt c* - **1** crystals, which belonged to trigonal space group $P3_221$ (Table S1, ESI†). The structure was solved by molecular replacement with one *cyt c* in the asymmetric unit. The *cyt c* fold was unaffected by foldamer binding (Fig. S4, ESI†). Electron density was evident for two molecules of **1** arranged as a stack, similar in dimension to *cyt c* (Fig. 1). Left-handed *M*-helicity was assigned unambiguously to both foldamers.

In the stack, one foldamer was well-defined with the N-terminal quinoline packed against the protein at Pro25 and Lys27. The other foldamer was modelled in opposite orientations (each 50% occupancy; Fig. S5, ESI†), arranged head-to-head or head-to-tail relative to the well-defined foldamer. Zinc ions were modelled at three separate sites involving His33, His39 or the foldamer–foldamer interface (Fig. 1 and Fig. S6, S7, ESI†).

The curved surface of the cylindrical foldamer stack is anionic owing to the sulfonates whereas the ends are mostly hydrophobic (Fig. S5B, ESI†). Notwithstanding the 2.1 Å resolution, close inspection of the crystal packing reveals multiple salt bridge interactions. In the well-defined foldamer, seven of the eight sulfonates make salt bridges to five lysine side chains ($N^{\epsilon} \cdots O-S = 2.8\text{--}3.4$ Å) in four neighbouring proteins (Fig. 2B). Lys5 and Lys73 are salt bridged to two sulfonates while Lys86, Lys87 and Lys100 each interact with one sulfonate. Interestingly, Lys5 binds the N-terminal quinoline (the cylinder base) in combination with Pro25 and Lys27 from a neighbouring protein (Fig. 2B). These contacts among others may have stabilized **1** in a single

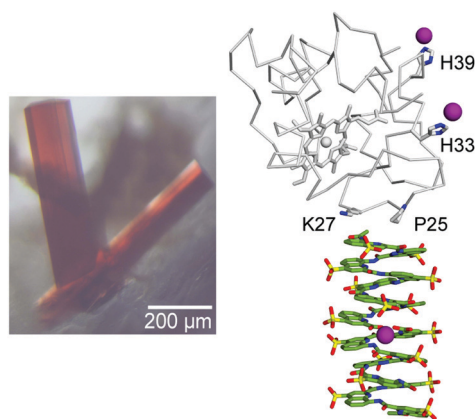


Fig. 1 Diffraction-quality *cyt c* - **1** co-crystals. The asymmetric unit comprised one *cyt c* and a stack of two foldamers (PDB id 6s8y). Purple spheres indicate zinc ions.

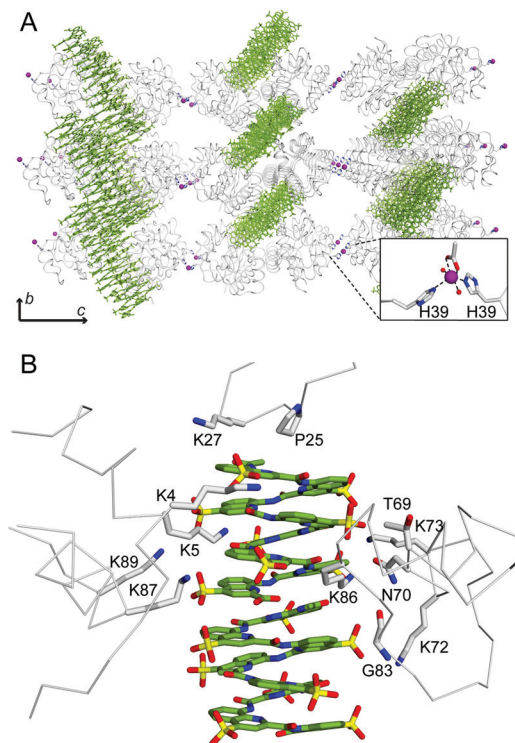


Fig. 2 (A) Crystal packing involved a ~5 nm cylinder comprising 4 foldamers. A bridging zinc ion at His39 mediated assembly (inset). (B) Protein–foldamer interfaces. The limited interactions of the second foldamer are evident, consistent with orientational disorder.

orientation and more importantly, selected the *M*-helix. Previously, it was observed that in a stack of three foldamers the central foldamer (lacking a tether for HCA binding) had negligible protein interactions and was present in two orientations.^{4d} In the current structure the well-ordered foldamer interacted with four protein surfaces, while the poorly-ordered foldamer interacted with just two proteins.

We considered the protein–foldamer interactions in terms of their interface areas. The 2 kDa foldamer **1** with a 1300 Å² surface area might be expected to form large interfaces with the protein. However, in the crystal, the well-defined foldamer formed small interfaces, ranging in size from 100 to 180 Å² with four neighbouring proteins (Fig. 2). The other foldamer formed only two significant interfaces of 165 or 190 Å² with *cyt c*, which apparently was insufficient to dictate its orientation. With <30% of its surface involved, this foldamer was bound weakly. All of these interfaces were smaller than the main protein–protein (270 Å²) and foldamer–foldamer (220 Å²) interfaces. The similarity with typical protein crystal packing interfaces¹⁸ suggests that the protein–foldamer contacts are weak and non-specific. Furthermore, the interface areas were comparable to those in protein–calix[4]arene complexes (200 Å²).^{14,15} The considerably smaller calix[4]arenes (0.8 kDa) bear a cavity that encapsulates individual lysine residues leading to larger interface areas compared to the foldamer.

Comparisons with sulfonatocalix[8]arene (**sclx₈**, 1.5 kDa)^{2b} and suramin (1.3 kDa)^{5b} are also informative. While the largest

cyt *c* – 1 interface is 190 Å², cyt *c* – **scix**₈ interfaces range from 400 to 550 Å², as the calixarene moulds to the protein surface. The even more flexible suramin forms interfaces up to 750 Å². Although smaller than foldamer **1**, the calixarenes and suramin form larger interfaces, facilitating their ‘molecular glue’ activity. The compactness and relative rigidity of the helical foldamer may diminish this ability. Nevertheless, the foldamer nestles between four protein chains where its anionic surface complements the cationic patches of the surrounding proteins (Fig. 2). The foldamer stack comprises 4 molecules in total, resulting in a ~4.6 nm long cylinder with a formal net charge of 36. The surrounding 8 molecules of cyt *c* are bound loosely (small interfaces) and the overall structure has large channels and a 50% solvent content (Fig. 2A). The role of zinc is noteworthy as it bridges cyt *c* molecules *via* His39 coordination. Zinc is prevalent in protein crystal structures as a mediator of assembly.¹⁹

Compound **1** lacks stereogenic centres and is synthesized as a racemic mixture of *P* and *M* conformers. Helix handedness inversion in water is extremely slow for such quinoline-based octamers.¹⁷ Therefore, the exclusive occurrence of the *M* conformer of **1** in the crystal structure amounts to a spontaneous chiral resolution. The resolution of racemic mixtures of chiral acids upon crystallization with a chiral base is well-established.²⁰ However, chiral resolution between molecules as large as a protein and a helical foldamer is, to the best of our knowledge, unprecedented. It reflects diastereoselective interactions in the solid state that presumably are preceded by similar interactions in solution. We attempted to observe handedness selection in solution by circular dichroism using analogue **2**. In this oligoamide, three quinoline monomers were substituted by aminomethyl-pyridine units (*P*, Scheme 1, see ESI† synthesis^{13,17}). These flexible units enhance the kinetics of helix handedness inversion making it possible to observe handedness bias in solution due to preferential interactions between one conformer and the protein.¹⁷ *P* monomers are isosteric to *Q* (*i.e.* the same inner rim) but have additional rotatable bonds (increased flexibility), and lack side chain functionality.

It was not possible to monitor solution interactions between cyt *c* and **2** in the same buffer used to grow the co-crystals with **1**. Under these conditions, co-precipitation with **2** occurred. Raising the pH to 5.4 and the addition of 25 mM sodium chloride facilitated solubility. Equilibration of **2** in the presence of cyt *c* revealed a positive band in the quinoline absorption region indicative of *P*-helicity, which remained unchanged over 72 h (Fig. 3). This band confirms diastereoselective interactions between **2** and cyt *c* in solution. In contrast to earlier investigations,^{4b,d} this selection occurs in the absence of any tether between the foldamer and the protein. However, the preferred handedness is opposite to that of **1** in the crystal structure. This change may be the result of the different conditions used (*e.g.* pH, zinc acetate) or structural differences between **1** and **2**. Another explanation may be that the strongest interactions in solution are not those that favoured crystal growth, *i.e.* different binding modes in solution and in the solid state.

NMR spectroscopy provided further insight into cyt *c* recognition by foldamer **1** (see ESI† methods). ¹H–¹⁵N HSQC-monitored titrations revealed increasing chemical shift perturbations ($\Delta\delta$) and

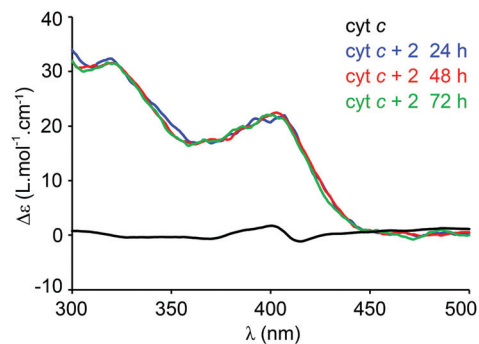


Fig. 3 CD spectra of the cyt *c* – **2** mixture after equilibration at 20 °C. The sample contained 0.09 mM protein–foldamer complex in 25 mM sodium acetate, 25 mM sodium chloride at pH 5.4.

some broadening as a function of the foldamer concentration, consistent with fast-to-intermediate exchange (Fig. 4A). The binding site in solution was a contiguous patch of ~20 residues, which was significantly different to the patches observed in the crystal structure (Fig. 4B and Fig. S8, ESI†). For example, Lys11 and Thr12 do not bind **1** in the crystal but their amide resonances were shifted and broadened at 2 eq. foldamer. Differences in the NMR and X-ray binding sites (Fig. S8, ESI†) are likely due to reorganization during crystallization, in favour of the site around Lys27, and facilitated by the zinc-mediated assembly (Fig. 2A). Interestingly, the NMR-defined binding site for the foldamer is similar to typical cyt *c* – calix[4]arene complexes.¹⁴ This observation suggests that sulfonate–lysine interactions direct complexation (electrostatic steering). The lysine-rich patch of cyt *c* is also prominent in binding protein partners in solution.²¹

The cyt *c* – 1 crystal structure is an assembly of two entities that differ strikingly in their chemical nature, size and shape.

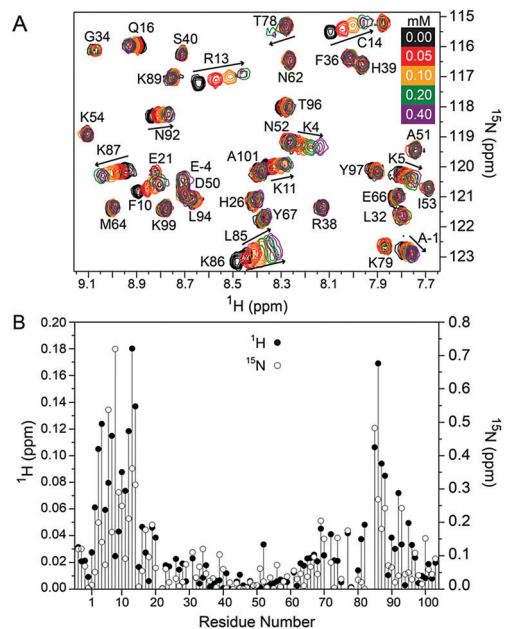


Fig. 4 (A) ¹H–¹⁵N HSQC titration of cyt *c* with **1** (coloured scale). (B) Chemical shift perturbations for cyt *c* backbone amides in the presence of 0.4 mM foldamer. Blanks correspond to unassigned or broadened resonances.

One is a highly cationic and globular biopolymer, the other is an anionic and helical synthetic ligand. The crystal composition of two foldamers (~4 kDa total) per protein (~13 kDa), results in a 1 : 3 mass ratio of synthetic to biological molecules. Charge-charge complementarity appears to facilitate the protein-foldamer interaction, highlighting the 'molecular glue' potential of foldamers to mediate interfaces and assembly. In view of these features, the $c-1$ complex may be considered as a biohybrid material.¹⁶ In the crystal, a cylindrical stack of four foldamers interacted with eight proteins *via* small interfaces, suggestive of weak interactions. While in solution a different binding mode occurred. The relatively compact and smooth surface of the foldamer precludes interdigitation with protein side chains. More extensive interactions with the protein surface may be achieved by a foldamer with alkyl (-R) or alkoxy (-OR; R = -CH₃ or -C₂H₅) linkers to the sulfonate substituents.

The property of **1** to mediate protein assembly by interacting with several surfaces hints at its application as a 'molecular glue'.^{2,14,22} Owing to the ease of functionalization, foldamers can be tailored according to the chemistry of the target protein.^{4b,d,g,11} For example, the replacement of sulfonate with amino substituents¹² may facilitate recognition and assembly of anionic proteins. Finally, this study highlights the potential of quinoline oligoamides to generate protein-based composite materials, for applications in therapeutics, sensors and nano-architectures.^{4b,d,g,10e,16}

This research was supported by NUI Galway (Hardiman Research Scholarship to JMA), the China Scholarship Council (pre-doctoral fellowship to XH), the European Union's Seventh Framework Programme (ERC-2012-AdG-320892 to IH) and Science Foundation Ireland (13/CDA/2168 to PBC). We thank SOLEIL synchrotron (France) for beam time allocation and the staff at beamline PROXIMA-2A for their assistance with data collection.

Conflicts of interest

There are no conflicts to declare.

Notes and references

- (a) S. van Dun, C. Ottmann, L. G. Milroy and L. Brunsveld, *J. Am. Chem. Soc.*, 2017, **139**, 13960; (b) S. L. Kuan, F. R. G. Bergamini and T. Weil, *Chem. Soc. Rev.*, 2018, **47**, 9069.
- (a) M. L. Rennie, A. M. Doolan, C. L. Raston and P. B. Crowley, *Angew. Chem., Int. Ed.*, 2017, **56**, 5517; (b) M. L. Rennie, G. C. Fox, J. Pérez and P. B. Crowley, *Angew. Chem., Int. Ed.*, 2018, **57**, 13764; (c) J. M. Alex, M. L. Rennie, S. Engilberge, G. Lehoczki, H. Dorotyya, A. Fizil, G. Batta and P. B. Crowley, *IUCr*, 2019, **6**, 238; (d) S. Engilberge, M. L. Rennie and P. B. Crowley, *FEBS Lett.*, 2019, DOI: 10.1002/1873-3468.13512.
- (a) P. J. de Vink, J. M. Briels, T. Schrader, L. G. Milroy, L. Brunsveld and C. Ottmann, *Angew. Chem., Int. Ed.*, 2017, **56**, 8998; (b) F. Guagnini, P. M. Antonik, M. L. Rennie, P. O'Byrne, A. R. Khan, R. Pinalli, E. Dalcanale and P. B. Crowley, *Angew. Chem., Int. Ed.*, 2018, **57**, 7126.
- (a) J. T. Ernst, J. Becerril, H. S. Park, H. Yin and A. D. Hamilton, *Angew. Chem., Int. Ed.*, 2003, **42**, 535; (b) J. Buratto, C. Colombo, M. Stupfel, S. J. Dawson, C. Dolain, B. Langlois d'Estaintot, L. Fischer, T. Granier, M. Laguerre, B. Gallois and I. Huc, *Angew. Chem., Int. Ed.*, 2014, **53**, 883; (c) S. Kumar, M. Birol, D. E. Schlamadinger, S. P. Wojcik, E. Rhoades and A. D. Miranker, *Nat. Commun.*, 2016, **25**, e11412; (d) M. Jewginski, T. Granier, B. Langlois d'Estaintot, L. Fischer, C. D. Mackereth and I. Huc, *J. Am. Chem. Soc.*, 2017, **139**, 2928; (e) D. Maity, S. Kumar, F. Curreli, A. K. Debnath and A. D. Hamilton, *Chem. - Eur. J.*, 2019, **25**, 7265; (f) Z. Hegeudus, C. M. Grison, J. A. Miles, S. Rodriguez-Marin, S. L. Warriner, M. E. Webb and A. J. Wilson, *Chem. Sci.*, 2019, **10**, 3956; (g) P. S. Reddy, B. L. d'Estaintot, T. Granier, C. D. Mackereth, L. Fischer and I. Huc, *Chem. - Eur. J.*, 2019, **25**, 11042.
- (a) C. Ren, K. Morohashi, A. N. Plotnikov, J. Jakoncic, S. G. Smith, J. Li, L. Zeng, Y. Rodriguez, V. Stojanoff, M. Walsh and M.-M. Zhou, *Chem. Biol.*, 2015, **22**, 161; (b) G. H. M. Salvador, T. R. Dreyer, A. A. S. Gomes, W. L. G. Cavalcante, J. I. dos Santos, C. A. Gandin, M. de Oliveira Neto, M. Gallacci and M. R. M. Fontes, *Sci. Rep.*, 2018, **8**, e10317.
- (a) D. Bier, S. Mittal, K. Bravo-Rodriguez, A. Sowislok, X. Guillory, J. Briels, C. Heid, M. Bartel, B. Wettig, L. Brunsveld, E. Sanchez-Garcia, T. Schrader and C. Ottmann, *J. Am. Chem. Soc.*, 2017, **139**, 16256; (b) C. Heid, A. Sowislok, T. Schaller, F. Niemeyer, F.-G. Klärner and T. Schrader, *Chem. - Eur. J.*, 2018, **24**, 11332.
- (a) D. J. Hill, M. J. Mio, R. B. Prince, T. S. Hughes and J. S. Moore, *Chem. Rev.*, 2001, **101**, 3893; (b) J. W. Checco and S. H. Gellman, *Curr. Opin. Struct. Biol.*, 2016, **39**, 96.
- (a) C. M. Goodman, S. Choi, S. Shandler and W. F. DeGrado, *Nat. Chem. Biol.*, 2007, **3**, 252; (b) J. W. Checco, D. F. Kreidler, N. C. Thomas, D. G. Belair, N. J. Rettko, W. L. Murphy, K. T. Forest and S. H. Gellman, *Proc. Natl. Acad. Sci. U. S. A.*, 2015, **112**, 4552.
- (a) D. W. Zhang, X. Zhao, J. L. Hou and Z. T. Li, *Chem. Rev.*, 2012, **112**, 5271; (b) Y. Ferrand and I. Huc, *Acc. Chem. Res.*, 2018, **51**, 970-977.
- (a) G. Guichard and I. Huc, *Chem. Commun.*, 2011, **47**, 5933; (b) C. Tsiamantas, S. J. Dawson and I. Huc, *C. R. Chim.*, 2016, **19**, 132; (c) Z. Lockhart and P. C. Knipe, *Angew. Chem., Int. Ed.*, 2018, **130**, 8614; (d) C. Lang, X. Deng, F. Yang, B. Yang, W. Wang, S. Qi, X. Zhang, C. Zhang, Z. Dong and J. Liu, *Angew. Chem., Int. Ed.*, 2017, **56**, 12668; (e) B. Gole, B. Kauffmann, V. Maurizot, I. Huc and Y. Ferrand, *Angew. Chem., Int. Ed.*, 2019, **58**, 8063; (f) J. M. Rogers, S. Kwon, S. J. Dawson, P. K. Mandal, H. Suga and I. Huc, *Nat. Chem.*, 2018, **10**, 405.
- M. Vallade, M. Jewginski, L. Fischer, J. Buratto, K. Bathany, J. M. Schmitter, M. Stupfel, F. Godde, C. D. Mackereth and I. Huc, *Bioconjugate Chem.*, 2018, **30**, 54.
- P. K. Mandal, B. Baptiste, B. L. d'Estaintot, B. Kauffmann and I. Huc, *ChemBioChem*, 2016, **17**, 1911.
- X. Hu, S. J. Dawson, P. K. Mandal, X. de Hatten, B. Baptiste and I. Huc, *Chem. Sci.*, 2017, **1**, 3741.
- (a) R. E. McGovern, H. Fernandes, A. R. Khan, N. P. Power and P. B. Crowley, *Nat. Chem.*, 2012, **4**, 527; (b) A. M. Doolan, M. L. Rennie and P. B. Crowley, *Chem. - Eur. J.*, 2018, **24**, 984.
- J. M. Alex, M. L. Rennie, S. Volpi, F. Sansone, A. Casnati and P. B. Crowley, *Cryst. Growth Des.*, 2018, **18**, 2467.
- X. Hu, P. Cebe, A. S. Weiss, F. Omenetto and D. L. Kaplan, *Mater. Today*, 2012, **15**, 208.
- M. Vallade, P. S. Reddy, L. Fischer and I. Huc, *Eur. J. Org. Chem.*, 2018, 5489.
- J. Janin, R. P. Bahadur and P. Chakrabarti, *Q. Rev. Biophys.*, 2008, **41**, 133.
- (a) P. B. Crowley, P. M. Matias, A. R. Khan, M. Roessle and D. I. Svergun, *Chem. - Eur. J.*, 2009, **15**, 12672; (b) L. A. Churchfield, R. G. Alberstein, L. M. Williamson and F. A. Tezcan, *J. Am. Chem. Soc.*, 2018, **140**, 10043.
- J. Jacques, A. Collet and S. H. Wilen, *Enantiomers, racemates and resolutions*, Krieger, Malabar, 3rd edn, 1994.
- (a) P. B. Crowley, K. S. Rabe, J. A. R. Worrall, G. W. Canters and M. Ubbink, *ChemBioChem*, 2002, **3**, 526; (b) P. B. Crowley and M. A. Carrondo, *Proteins*, 2004, **55**, 603; (c) A. N. Volkov, Q. Bashir, J. A. R. Worrall, G. M. Ullmann and M. Ubbink, *J. Am. Chem. Soc.*, 2010, **132**, 11487.
- S. Engilberge, F. Riobé, T. Wagner, S. D. Pietro, C. Breyton, B. Franzetti, S. Shima, E. Girard, E. Dumont and O. Maury, *Chem. - Eur. J.*, 2018, **24**, 9739.